Carbohydrate Polymers 114 (2014) 537–545

Contents lists available at ScienceDirect

Carbohydrate Polymers

journal homepage: www.elsevier.com/locate/carbpol

# Preparation and properties of self-reinforced cellulose composite films from Agave microfibrils using an ionic liquid

K. Obi Reddy [a,*], Jinming Zhang [b], Jun Zhang [b], A. Varada Rajulu [c]

[a] Department of Chemical Engineering Technology, Doornfontein Campus, University of Johannesburg, P.O. Box 17011, Johannesburg 2028, South Africa
[b] CAS Key Lab of Engineering Plastics, Institute of Chemistry, Chinese Academy of Sciences (CAS), Beijing, China
[c] Department of Physics, Osmania University, Hyderabad 500007, India

ARTICLE INFO

*Article history:*
Received 10 June 2014
Received in revised form 18 August 2014
Accepted 22 August 2014
Available online 30 August 2014

*Keywords:*
Agave fibers
Cellulose microfibrils
Ionic liquid
Regenerated cellulose
Spectroscopy
Crystallinity

ABSTRACT

The applications of natural fibers and their microfibrils are increasing rapidly due to their environment benefits, specific strength properties and renewability. In the present work, we successfully extracted cellulose microfibrils from Agave natural fibers by chemical method. The extracted microfibrils were characterized by chemical analysis. The cellulose microfibrils were found to dissolve in an ionic liquid 1-allyl-3-methylimidazolium chloride (AmimCl) to larger extent along with little quantity of undissolved microfibrils. Using this solution, the self-reinforced regenerated cellulose composite films were prepared. The raw fiber, extracted cellulose microfibrils and regenerated cellulose composite films were characterized by FTIR, $^{13}C$ CP-MAS NMR, XRD, TGA and SEM techniques. The average tensile strength, modulus and elongation at break of the self-reinforced cellulose composite films were found to be 135 MPa, 8150 MPa and 3.2%, respectively. The high values of tensile strength and modulus were attributed to the self-reinforcement of Agave fibers in their generated matrix. These self-reinforced cellulose biodegradable composite films prepared from renewable source can find applications in packaging field.


## 1. Introduction

Recently, biomass-derived biodegradable flexible and apparent films, which are mostly based on cellulose, starch, protein, chitosan or their derivatives, have fascinated much attention because of their potential to substitute conventional petro-chemical products in many aspects (Biswas, Saha, Lawton, Shogren, & Willett, 2006; Pelissari, Grossmann, Yamashita, & Pineda, 2009; Yang et al., 2014). Cellulose is the world's most common biopolymer and is measured as an almost never-ending source of raw material for the rising demand of environmentally gracious and biocompatible products (Eichhorn, 2011; Klemm et al., 2011). It has drawn much attention due to its unique properties such as low density simultaneously with high mechanical strength, low cost, renewability, biodegradability, good film-forming performance, chemical stability and enormous of chemical derivations (Klemm, Heublein, Fink, & Bohn, 2005). There are several natural sources of cellulose; plants (major sources are wood and cotton), aerobic bacteria and some animals (tunicates). It has attracted more and more attention as a renewable resource for applications in the fields of material and energy (Eichhorn, 2011; Klemm et al., 2011).

Cellulose is a linear polysaccharide composed of β-1-4-linked D-glucopyranose repeating units. Due to its many hydroxyl groups and to its tacticity, cellulose forms strong intra- and inter-molecular hydrogen bonds, giving rise to its three dimensional, supra-molecular and semicrystalline structures (Eichhorn, 2011). However, on description of the extensive bulky network linking hydrogen bonds and partially crystal structure, cellulose cannot be dissolved in water or most usual organic solvents (Soheilmoghaddam et al., 2014), which restricts its potential applications in forming processes. Several solvent systems have been developed to dissolve regenerated cellulose materials, such as NaOH/$CS_2$ (Hyden, 1929), lithium chloride/*N,N*-dimethylacetamide (LiCl/DMAc) (McCormick, Callais, & Hutchinson, 1985), *N*-methylmorpholine-*N*-oxide (NMMO) (Fink, Weigel, Purz, & Ganster, 2001), phosphoric acid (Northolt et al., 2001), LiOH/urea and NaOH/urea (Cai & Zhang, 2005) and ionic liquids (Kosan, Michels, & Meister, 2008). However, ionic liquid (IL) has been gaining interest because of its potential to regenerate and chemically modify the cellulose over the other process (Swatloski, Spear, Holbrey, & Rogers, 2002; Zhu et al., 2006). Further, ionic liquids are characterized by excellent dissolubility, low toxicity, thermal stability, near zero volatility and recyclability

* Corresponding author. Tel.: +27 846 606 269.
*E-mail addresses:* obireddyk80@gmail.com, obik@uj.ac.za (K.O. Reddy).

http://dx.doi.org/10.1016/j.carbpol.2014.08.054
0144-8617/

(Hameed, Guo, Tay, & Kazarian, 2011). Literature has indicated the availability of a variety of ionic liquid solvents for the production of regenerated cellulose from biomass (Cao, Li, Zhang, Zhang, & He, 2010; Casas et al., 2012; Fort et al., 2007; Jiang et al., 2011).

Recent efforts have converted cellulose (obtained from biomass) to several forms like cellulose microfibrils, micro crystalline cellulose, nanocellulose, fibrillated nanocellulose and nanocellulose whiskers with several end use applications (Eichhorn, 2011; Janardhnan & Sain, 2007; Maheswari, Reddy, Muzenda, Guduri, & Rajulu, 2012; Orts et al., 2005; Samir, Alloin, & Dufresne, 2005; Siro & Plackett, 2010; Taniguchi & Okamura, 1998). However, the consumption of energy to produce cellulose microfibrils is much lower than that of other cellulose derives. The microfibers are intended to be used in numerous applications varying from constituent part for plastic reinforcement, to gel forming food or cosmetic additives for their gelling, thickening properties in water and medical products (Lowys, Desbrieres, & Rinaudo, 2001; Mouro et al., 2003; Nakagaito & Yano, 2005).

The natural Agave fibers were selected in this work to extract cellulose microfibrils. Agave (also called century plant) belongs to the Agavaceae family of *Agave americana* L. species. Though this plant is native to Mexico and other parts of the Caribbean area, it is now cultivated worldwide as an ornamental plant (Msahli, Sakli, & Drean, 2006). It is widely used to make ropes and twines for agricultural purposes. In an earlier work, the authors reported the structural and physical properties of Agave fibers (Reddy, Reddy, Zhang, Zhang, & Varada Rajulu, 2013). In this study, chemical treatments including acid-chlorite, alkaline and acid hydrolysis processes were used to produce cellulose microfibrils from Agave fibers. These microfibrils were found to dissolve in the ionic liquid (1-allyl-3-methylimidazolium chloride) (AmimCl) to a larger extent with minor quantity of undissolved microfibrils. Using this solution, regenerated cellulose composite films with self-reinforced microfibrils were prepared. The raw fibers, extracted microfibers and regenerated cellulose composite film were characterized by chemical analysis, FTIR, $^{13}$CP-MAS NMR, X-ray diffraction, morphology and thermogravimetric techniques and tensile testing.

## 2. Experimental

### 2.1. Materials

*Agave* fibers used in this study were extracted from the mature leaves of the plant by the usual water retting with beating process according to previous work (Reddy et al., 2013). After extraction, fibers were cleaned with tap water to remove the unwanted materials from fibers. Finally extracted fibers were dried at room temperature for a week and stored in polyethylene bags. Acetic acid, ethanol, sodium bisulphite, sodium hydroxide pellets (Merck Chemicals), nitric acid, sodium chlorite and toluene (Sd-Fine Chemicals) chemicals used were of analytical grade.

### 2.2. Cellulose microfibrils extraction

Extracted and chopped Agave fibers were sieved through 250 mesh and dried at 105 °C for 24 h. Then the fibers were dewaxed by refluxing with toluene–ethanol (2:1, v/v) for 6 h in a Soxhlet apparatus. The dewaxed fiber samples were then delignified with 0.7% sodium chlorite at 100 °C for 2 h in acidic solution (pH 4–4.2 adjusted by 10% acetic acid) using a fiber to liquor ratio of 1:50. After being filtered and extensively washed with 2% sodium bisulphite and distilled water, the residue was dried at 105 °C in an oven until constant weight. The holocellulose was treated with 17.5% (w/v) NaOH solution at 20 °C for 45 min, filtered, washed with 10% acetic acid, distilled water and finally dried at 105 °C in an oven until constant weight. The extracted crude cellulose was treated with volume concentrations of 80% acetic acid −70% nitric acid taken in 10:1 ratio at 120 °C for 20 min. After being cooled, it was then washed sequentially with 95% ethanol and distilled water to remove excess of acid mixture. Finally, the purified cellulose microfibrils were dried at 105 °C in an oven until constant weight. The above procedure of extraction of cellulose microfibrils was adopted from Maheswari et al. (2012).

### 2.3. Chemical analysis

The chemical composition of Agave raw fibers and extracted cellulose microfibrils was determined using the standard TAPPI (Technical Association of the Pulp and Paper Associations) methods for different components, namely: T 204 cm-07 for extractives, T 203 cm-99 for α-cellulose, T 222 om-06 for lignin and T 211 om-07 for ash content. The holocellulose was determined according to the method described by Wise, Murphy, and D'Addieco (1946). The hemicellulose fraction was calculated as the difference between the holocellulose and α-cellulose content. The percent contents of α-cellulose, hemicellulose and lignin were determined, and based on five samples the average and standard deviation values are reported.

### 2.4. Dissolution and regeneration of cellulose film

A distinct tentative process for preparation of regenerated cellulose films with ionic liquid was as follows. First, the extracted cellulose microfibrils sample was added into a round bottom flask containing AmimCl with a weight ratio of 4 wt% (cellulose microfibrils to AmimCl). The mixture of cellulose microfibrils/AmimCl was stirred continuously in an oil bath at 80 °C with nitrogen atmosphere to form a solution having larger amounts of dissolved microfibrils and a little amount of undissolved microfibrils and then degassed. After that, the regenerated cellulose composite films were prepared by casting the homogeneous mixture on glass plate. Then, the regenerated cellulose composite films were soaked in deionized water and washed thoroughly to remove ionic liquid (no $Cl^-$ ions were detectable by the $AgNO_3$ test). The obtained regenerated cellulose composite films were dried in air for 48 h and stored in vacuum desiccators prior to characterization. These films were found to be stable even after immersion in water for two days.

### 2.5. FTIR spectroscopy

Fourier transform-infrared spectroscopy studies of raw fibers, extracted cellulose microfibrils and the regenerated cellulose composite films were carried out using a Smart iTR ATR Nicolet iS 10 FT-IR spectrophotometer. All the spectra were recorded in the 4000–500 $cm^{-1}$ region with 32 scans in each case, at a resolution of 4 $cm^{-1}$.

### 2.6. NMR (CP-MAS) spectroscopy

$^{13}$C cross-polarization magic angle spinning (CP-MAS) nuclear magnetic resonance (NMR) spectra of raw fiber, extracted cellulose microfibrils and the regenerated cellulose composite films were run on a Bruker DSX 300 MHz solid-state NMR spectrometer. The operating frequency for $^{13}$C nuclei was fixed at 75.46 MHz, and the samples filled in 5 mm rotor were spun at a rate of 5 kHz at room temperature.

### 2.7. X-ray diffraction analysis

Wide-angle X-ray diffractograms of raw fibers, extracted cellulose microfibrils and the regenerated cellulose composite films were recorded on a Rigaku Ultima IV X-ray diffractometer. The system has a rotating anode generator with a copper target and a wide-angle powder goniometer. The generator was operated at 40 kV power using filtered Cu $K\alpha$ radiation ($\lambda = 1.5406$ Å) and 30 mA, and the samples were scanned in the $2\theta$ range of 5–50°. The crystallinity index (CrI) was calculated by Segal's method (Segal, Creely, Martin, & Conrad, 1959) using the following equation:

$$CrI = \left[\frac{Ihkl - Iam}{Ihkl}\right] \times 100\%$$

where *Ihkl* is the intensity of diffraction maximum of crystalline regions [I200 (22.8°) in cellulose I; I200 (21.9°) in cellulose II], while *Iam* is the intensity value for the amorphous cellulose close to 17.3° (Sèbe, Ham-Pichavant, Ibarboure, Koffi, & Tingaut, 2012).

### 2.8. Thermogravimetric analysis

The thermal stability of Agave raw fibers, extracted cellulose micro fibrils and regenerated cellulose composite films were established using a thermogravimetric analyzer (Perkin Elmer TGA-7). The amount of sample for each measurement was about 10 mg. All the measurements were performed under a nitrogen atmosphere with a gas flow of 100 mL/min and heated from 50 to 600 °C at a rate of 10 °C/min.

### 2.9. Morphology

Scanning electron microscope (JEOL JSM 820) was used to study the morphology of raw fiber, extracted cellulose microfibrils and regenerated cellulose composite film. The samples were gold coated prior to recording the micrographs. The acceleration voltage was set at 5 kV.

### 2.10. Tensile testing

An Universal testing machine (Instron 3369) with a 10 kN loaded cell was used to determine the tensile strength, Young's modulus and elongation at break of the films at a constant extension speed of 5 mm/min. regenerated cellulose composite films were cut into rectangular shape with a length of 100 mm and a width of 10 mm, and were then clipped by two clamps on instrument. Five specimens were used for tensile test and the average values of tensile properties were reported. The tests were conducted at a temperature of 30 °C and relative humidity of 70%.

## 3. Results and discussion

### 3.1. Chemical analysis

The primary work concerned in the present research was to extract fibers from Agave leaves, subsequently convert them into cellulose microfibrils and characterize them. It was also planned to dissolve the microfibrils in an ionic liquid and make regenerated cellulose film. According to chemical analysis results, raw fibers contained 71.65% of α-cellulose, 22.24% of hemicellulose and 6.09% of lignin. The extracted cellulose microfibrils contained α-cellulose, hemicellulose and lignin contents in 93.3, 2.35 and 3.69%, respectively. From the chemical analysis, it is evident that the α-cellulose content increased while the lignin and hemicellulose decreased in the case of microfibrils when compared to the raw fibers. This may be attributed to the effect of chemicals that were used during the cellulose microfibrils extraction process. This proves that during the acidified sodium chlorite, sodium hydroxide and acid hydrolysis treatments significant breakdown of the ligno-cellulosic structure took place resulting in the hydrolysis of hemicellulose fraction and depolymerization of lignin. In order to further probe this, we also carried out FTIR and $^{13}C$ NMR (CP-MAS) analyses.

### 3.2. FTIR spectra analysis

The FTIR spectra of the Agave raw fiber, cellulose microfibrils and the regenerated cellulose composite film are shown in Fig. 1. From Fig. 1, it is evident that, the three spectra had well defined common bands at 3333, 2917, 1427, 1369, 1316, 1159, 1101, 1052, 1030 and 897 $cm^{-1}$ corresponding to cellulose (Liu et al., 2006; Sain & Panthapulakkal, 2006; Maheswari et al., 2012; Reddy et al., 2013). Further, an additional common band at around 1626 $cm^{-1}$ was found in all the three cases that was attributed to the bending mode of the absorbed water (Sain & Panthapulakkal, 2006). However, in the case of raw fibers, additional bands at around 1731, 1509, 1461 and 1243 $cm^{-1}$ were also present that were attributed to hemicellulose and lignin (Reddy, Guduri, & Rajulu, 2009; Maheswari et al., 2012; Reddy et al., 2013). The intensity of these bands decreased in the extracted cellulose microfibrils, because of the most of removal of hemicellulose and lignin by chemical treatments in cellulose extraction process. The similarity of FTIR spectra of the original cellulose microfibrils and regenerated cellulose composite film indicates that there was no effect of ionic liquid in cellulose structure. However, the intensity of the O—H stretching of cellulose microfibrils band was found to be very low as compared to the regenerated cellulose due to splitting of hydrogen bonds in the cellulose (Zhang, Wu, Zhang, & He, 2005). Therefore, it could be concluded that the regenerated cellulose was without any derivatization during the dissolution and regeneration processes.

### 3.3. $^{13}C$ CP-MAS NMR spectra analysis

The $^{13}C$ CP-MAS (cross-polarization magic angle spinning) NMR spectra for the raw fiber, cellulose microfibrils and regenerated cellulose composite film are shown in Fig. 2. The spectrum of raw fiber mainly shows the corresponding signals for the cellulose, hemicellulose, and lignin. The entire noticeable peaks of the cellulose carbon atoms occurred in the range of 60 to 110 ppm (Maheswari et al., 2012). The most prominent peaks of raw fiber were the superimposed C-2, C-3 and C-5 signals at 73.1–75.9 ppm, and other important features were C-1 (105.7 ppm), C-4 (89.7 ppm) and C-6 (65.8 ppm), while the peak at 84.4 ppm is due to the disordered C-4 carbon of cellulose (Reddy et al., 2009). The carbon peaks of the hemicellulose are expected at 103 ppm (C-1), 84 ppm (C-4), 72–75 ppm (C-2 and C-3) and 65 ppm (C-5), but the strong cellulose peaks overlapped these peaks (Maheswari et al., 2012). The spectrum of raw fiber shows a sharp moderate peak at 21.5 ppm, and a broad peak at 172.9 ppm. These peaks were attributed to the methyl and carboxylic carbons of acetyl groups in hemicellulose (Reddy et al., 2009). The lignin peaks appeared between 110 and 160 ppm, which were assigned to different aromatic carbons of lignin (Capanema, Balakshin, & Kadla, 2004; Nadji et al., 2009). In addition, the peak between 10 and 40 ppm was attributed to the methyl and alkyl carbons (including acetyl groups in hemicellulose), while the peak at 56.6 ppm was attributed to methoxyl (—$OCH_3$) and carbonyl groups, respectively, in lignin (Reddy et al., 2009). The extracted cellulose microfibrils (form raw fiber) spectrum (Fig. 2) indicated the disappearance of peaks at 110–160 ppm, 56.6 ppm and 10–40 ppm of lignin, as well as 21.5 and 172.9 ppm of hemicellulose indicating that most of hemicellulose and lignin were successfully removed as a result of the different chemical treatments by cellulose extraction

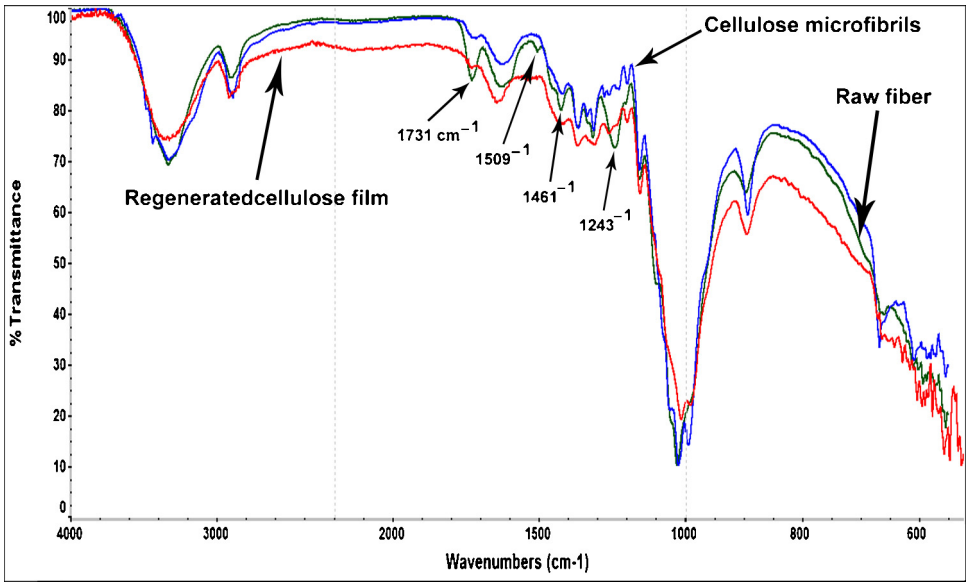


**Fig. 1.** FTIR spectra of raw fiber, extracted cellulose microfibrils and regenerated cellulose composite film.

process. While the other (cellulose) peaks, i.e., those appeared in the region 60–110 ppm almost remained the same. The NMR spectrum of regenerated cellulose composite film is also shown in Fig. 2. The inconsequential features of the spectrum of the deshielding of its chemical shift were observed which further indicates that there was no effect of ionic liquid in cellulose structure of regenerated films.

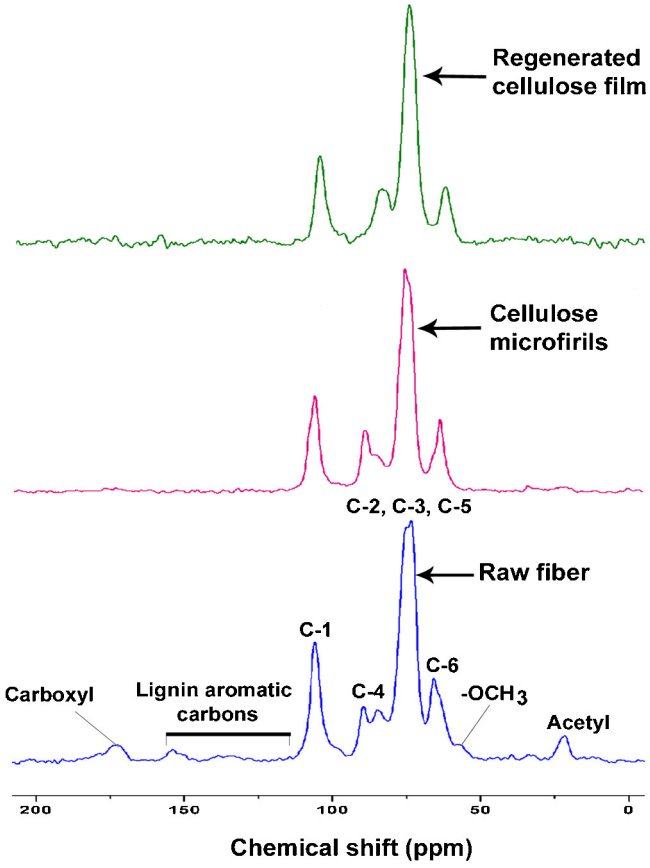


**Fig. 2.** NMR spectra of raw fiber, extracted cellulose microfibrils and regenerated cellulose composite film.

### 3.4. X-ray diffraction analysis

The crystallinity of the extracted cellulose was investigated by using XRD. Certainly, cellulose has a crystalline structure with respect to hemicellulose and lignin, which are amorphous in nature. More specifically, cellulose has a crystalline structure due to the hydrogen bond interactions and van der Waals forces between adjacent macromolecules (Zhang & Lynd, 2004). X-ray diffraction (XRD) analysis was used to evaluate the crystallinity of the raw fiber, extracted cellulose microfibrils and regenerated cellulose composite film. Though all the samples were semi-crystalline, the crystallinity was somewhat different among them. The XRD patterns of raw fiber, extracted cellulose microfibrils and regenerated cellulose composite film are shown in Fig. 3. The X-ray diffractogram of raw fiber shows a strong crystalline peak at 22.8° for (2 0 0) crystal plane, a small peak at 34.6° for (0 0 4) crystal plane, and a broad peak at 16.0° overlapped by 15.1° (1 −1 0) crystal plane and 16.8° (1 1 0) crystal plane, which indicate a cellulose I crystalline structure of raw fiber (Oh et al., 2005). In the extracted cellulose microfibrils (Fig. 3), a notably unique diffraction pattern assigned as the mixture of cellulose I and II was observed. Except the peaks of cellulose I, new peaks at $2\theta = 12.4°$ (1 −1 0), 20.1° (1 1 0) and 21.9° (2 0 0) appeared to indicate the formation of cellulose II. That is to say, the native cellulose (cellulose I) was partially transformed into cellulose II through the chemical extraction process of cellulose microfibrils. The diffractogram of the regenerated cellulose composite film indicated that the main diffraction peak appeared at 20–22° (cellulose II), with relatively low intensity, and the peak shape was broad. Further the subsidiary diffraction peaks (12.4°, 15.1°, 16.8° and 34.6°) were almost nonexistent. All of the phenomena indicated that the areas of crystal region became small, and the regenerated cellulose film mainly attained an amorphous structure. The calculated crystallinity index (CrI) values of raw fiber, extracted cellulose microfibrils and regenerated cellulose composite film were found to be 57.2, 64.4 and 55.9%, respectively. The crystallinity index of extracted cellulose microfibrils was found to be higher than the raw fiber and regenerated cellulose composite film due to the removal of non-cellulosic materials. During the hydrolysis process, hydronium ions can penetrate the more accessible amorphous regions of cellulose to allow the hydrolytic cleavage of glycosidic bonds. As a result, the raw fibers eventually release individual crystallites and these monocrystals are

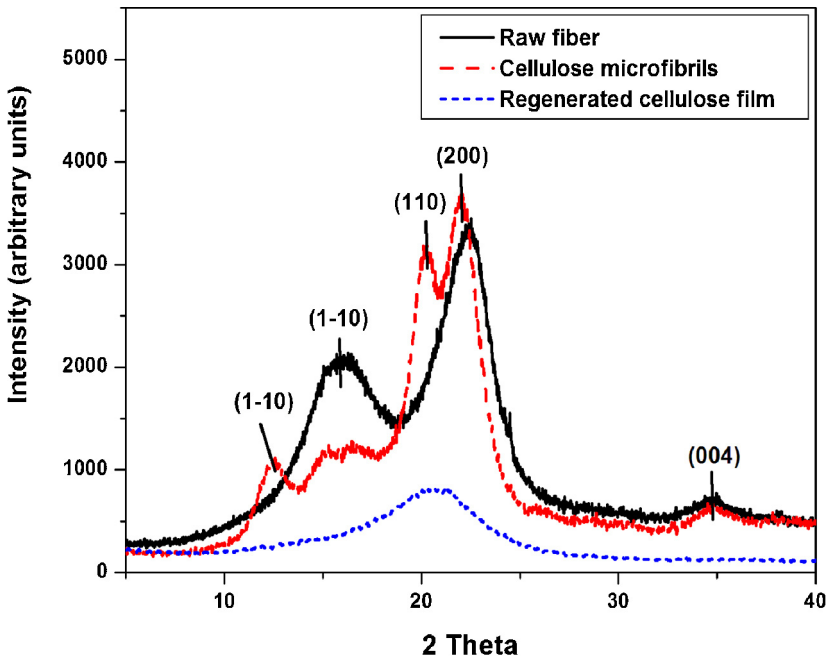


**Fig. 3.** X-Ray diffractograms of raw fiber, extracted cellulose microfibrils and regenerated cellulose composite film.

realigned, which improve the cellulose crystallinity (Johar, Ahmad, & Dufresne, 2012). The lower crystallinity in the regenerated cellulose composite film (Lee, Doherty, Linhardt, & Dordick, 2009) was probably caused by the rapid depolymerization of cellulose in the dissolving process (Zhang et al., 2005).

### 3.5. Thermogravimetric analysis

Thermogravimetric analysis (TGA) was deliberate to access the thermal stability of raw fiber, extracted cellulose microfibrils and regenerated cellulose composite film and the corresponding primary thermograms are shown in Fig. 4. The samples decomposition is exhibited in two stages, indicating the presence of three different constituents (Yang, Yan, Chen, Lee, & Zheng, 2007). The first decomposition stage was found in 250–350 °C temperature range for raw fiber. During this stage, thermal depolymerization of hemicelluloses and some fraction of lignin resulted besides destruction of crystalline regions of cellulose. These were then slowly transformed into $CO_2$ and volatile hydrocarbons. The weight loss in this temperature range was found to be 25%. The second degradation stage occurred in the range of 350–440 °C for raw fiber. The weight loss over these temperature ranges was found to be 56.5%. During this stage cellulose was almost completely burnt because of the continuing thermal oxidative degradation of the char produced. However, in the extracted cellulose microfibrils, the first degradation stage started in the region 280–370 °C and the corresponding

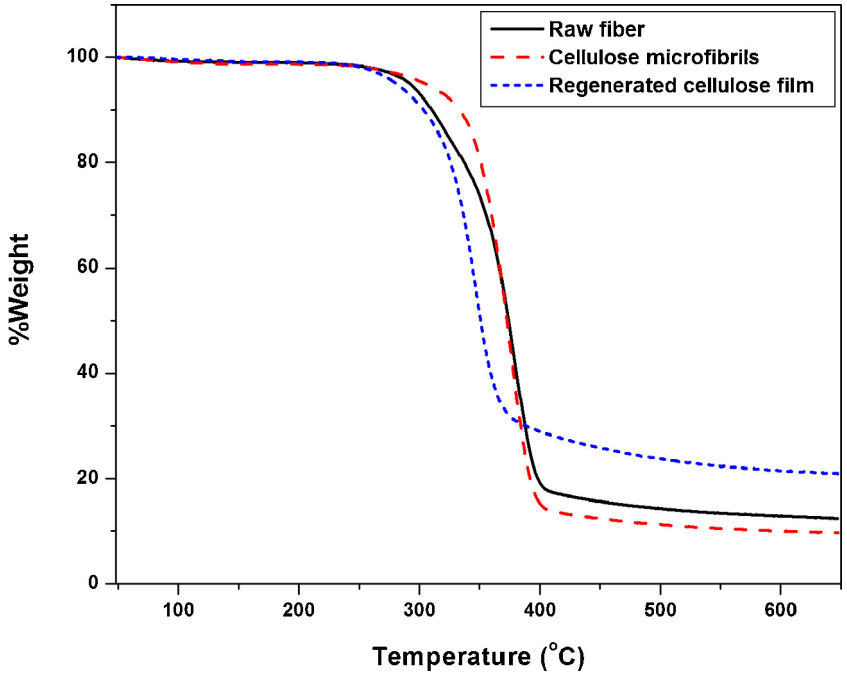


**Fig. 4.** Primary thermograms of raw fiber, extracted cellulose microfibrils and regenerated cellulose composite film.

weight loss in this temperature range was found to be 39%. These results clearly illustrate that the thermal stability of the extracted cellulose microfibrils was higher than that of the raw fibers. This was attributed to the removal of hemicellulose and lignin from the raw fibers on several chemical treatments. The second degradation stage started in the region 370–440 °C and the weight loss in this temperature was found to be 70%. Further for the regenerated cellulose composite film, the first and second degradation stages occurred in the regions 240–330 and 340–470 °C, respectively, with the corresponding weight loss of 23.6 and 50.8%, respectively. The lower thermal stability of regenerated cellulose composite film compared to the raw fiber and extracted cellulose microfibrils was due to the low crystallinity of regenerated cellulose. Similar results were reported during the dissolution of cellulose in ionic liquid (Swatloski et al., 2002; Liu et al., 2007; Li, Wu, Chen, Liu, & Sun, 2011). However, the char content of the regenerated cellulose composite was found to be higher than that of raw fiber and microfibrils.

### 3.6. Surface morphology

The morphology of raw century fibers and extracted cellulose microfibrils was studied using scanning electron microscope. Fig. 5 reveals the morphological changes between the raw Agave fibers and extracted cellulose microfibrils. The micrographs of raw century fiber surface shown in Fig. 5a and b reveal that the impurities were localized on the surface. Generally most of natural cellulose fibers are with multi cellular structure and then composed of cellulose surrounded and cemented together with lignin and hemicelluloses. In our earlier studies, the chemical composition and structural characterization of raw century (Agave) fibers were already reported (Reddy et al., 2013). Following the completion of several chemical treatments, most of the lignin and hemicellulose were removed to large extent and the cellulose microfibrils were separated from the raw fibers (from Fig. 5c and d). The micrographs also indicate a highly fibrous network-like structure consisting of cellulose microfibrils. It is clear from the micrographs that the range of diameter of the microfibrils was about 8–14 μm, which was lower than that of diameter of raw fibers (0.21 mm). In addition, some structures of bundled fibers are still detectable (Fig. 5c). At higher magnification (Fig. 5d), microfibrils appear to have a clean and rough surface. The morphological changes in the fiber surface were recognized to the removal of the hemicelluloses and lignin by chemical treatments.

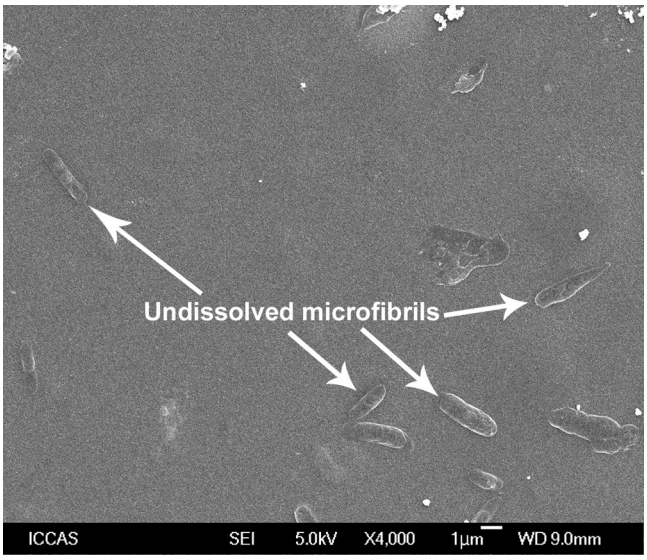


**Fig. 6.** Scanning electron micrograph of regenerated cellulose composite film surface.

As well, the morphology of produced regenerated cellulose composite film was analyzed by scanning electron microscopy (SEM), and the corresponding micrograph is shown in Fig. 6. It can be seen

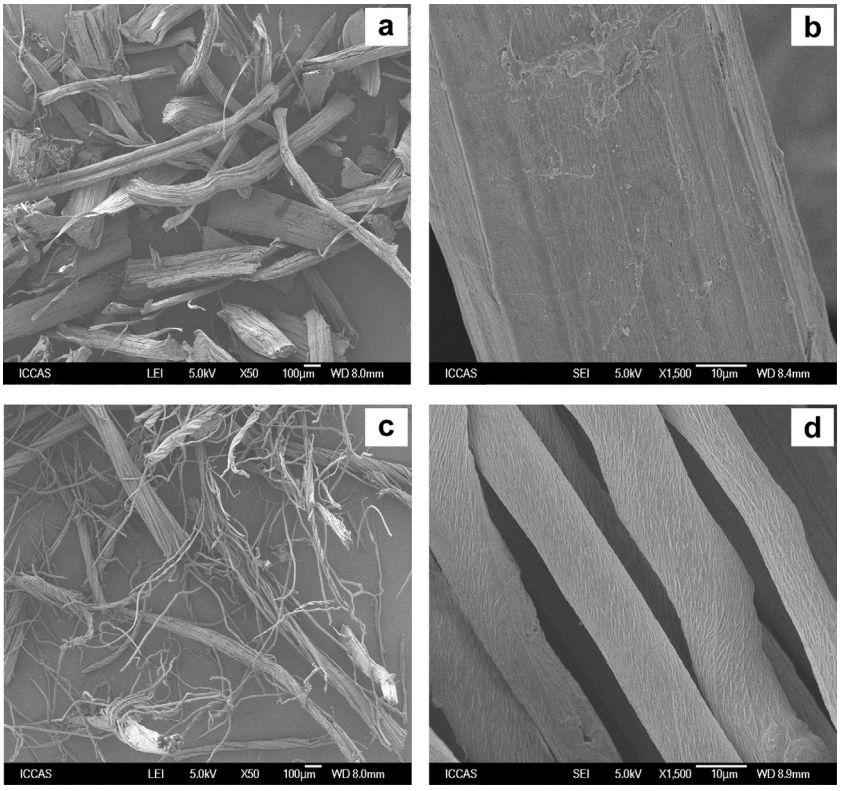


**Fig. 5.** Scanning electron micrographs raw fiber surfaces ((a) and (b)) and extracted cellulose microfibrils surface ((c) and (d)) at different magnifications.

**Table 1**
Comparison of tensile properties of regenerated cellulose composite film with various biopolymer films.

| Biopolymer films | Film preparation method | Tensile strength (MPa) | Tensile modulus (MPa) | Elongation at break (%) | References |
|---|---|---|---|---|---|
| Polylactic acid (PLA) | Solution casting | 16.8 | 1152 | 402 | Ashok et al. (2014) |
| Polyvinyl alcohol (PVA) | Solution casting | 83 | 1900 | 45 | Zhang et al. (2003) |
| Polypropylene carbonate (PPC) | Solution casting | 12.8 | 823 | 821 | Feng et al. (2014) |
| Polyhydroxybutyrate (PHBV) | Solution casting | 28.9 | 3570 | 10.2 | Cyras et al. (2007) |
| Banana starch (BS) | Solution casting | 5.01 | 46.86 | 14.30 | Torres et al. (2011) |
| Cassava starch (CS) | Solution casting | 2.56 | 30.27 | 43.45 | Torres et al. (2011) |
| Sweet potato starch (SPS) | Solution casting | 3.72 | 106.01 | 33.83 | Torres et al. (2011) |
| Chitosan (CH) | Solution casting | 8.4 | 134.6 | 19.6 | Pereda et al. (2014) |
| Regenerated cellulose (RC) | Solution casting | 135 | 8150 | 3.2 | Present work |

**Fig. 7.** Photograph of the regenerated cellulose composite film taken before a plant.

from SEM micrograph that regenerated cellulose composite film exhibited cellulose continuous phase along with cellulose microfibrils as the discontinuous phase. The presence of microfibrils in the composite film can be visualized in the micrograph. This further confirms the formation of all cellulose composite film. The visible fairly transparency and high flexibility of the regenerated cellulose casting film is demonstrated in Fig. 7.

### 3.7. Tensile properties

To evaluate the tensile properties of the regenerated cellulose composite film, the corresponding stress–strain curves of five film specimens are shown in Fig. 8. From Fig. 8, the regenerated cellulose film showed a behavior with stress increasing rapidly at small strains and more slowly after the yield point. The average tensile strength, Young's modulus and %elongation at break of the regenerated cellulose composite film were found to be $135 \pm 8$ MPa, $8150 \pm 257$ MPa and $3.2 \pm 0.2$%, respectively, which are higher than for the films made using cotton linters. In comparison, the tensile strength for the regenerated cellulose films obtained with AmimCl was higher than that of the largely used commercial polyolefin films, such as polypropylene (PP) and polyethylene (PE) with tensile strength in the range of 20–40 MPa (Ding, 1995).

The tensile properties of regenerated cellulose composite film were compared with those of other biopolymer films (Ashok et al., 2014; Cyras, Commisso, Mauri, & Vazquez, 2007; Feng et al., 2014; Pereda, Dufresne, Aranguren, & Marcovich, 2014; Torres, Troncoso, Torres, Díaz, & Amaya, 2011; Zhang et al., 2003) and are presented in Table 1. From this table, it can be observed that the tensile strength and tensile modulus of regenerated cellulose composite

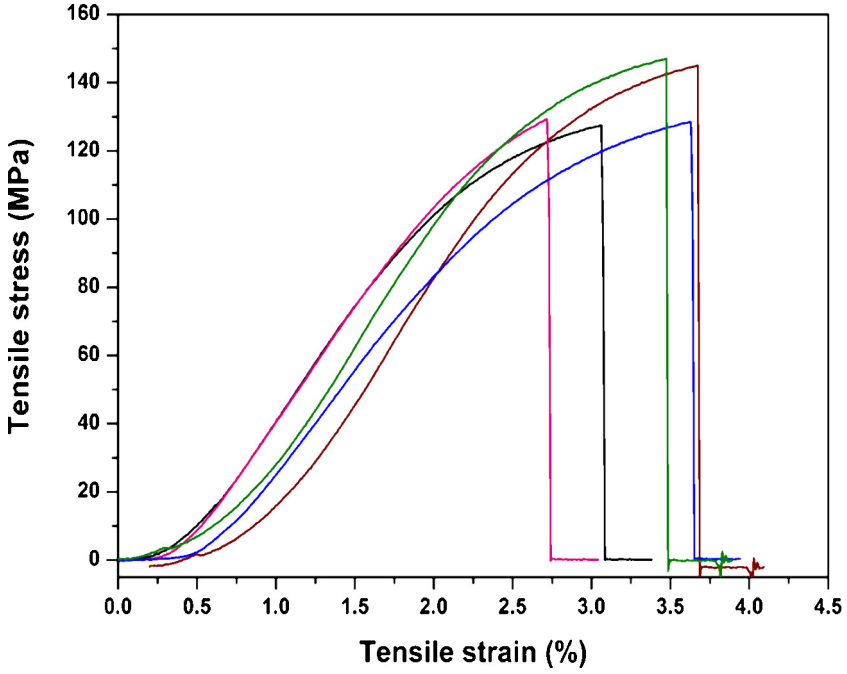


**Fig. 8.** Stress–strain curve of five regenerated cellulose composite film specimens.

film from Agave fiber were higher than other biopolymer films, while the elongation at break was lower than other biopolymer films. The increase in tensile strength and modulus of regenerated cellulose composite films could be due to the covalent bonding of soluble cellulose with insoluble cellulose microfibrils, which lead to an increase in the stiffness, which usually led to a decrease in the deformation capability of the regenerated cellulose composite films.

## 4. Conclusion

Agave leaf fibers are interesting alternative as cellulose source for several applications. This material is renewable and hugely available in many regions of the world. An effective and convenient chemical process was used to extract the cellulose microfibrils from Agave fibers. The Agave microfibrils were found to dissolve in the ionic liquid AmimCl to a very large extent with little amount of undissolved microfibrils. Using the solution, the regenerated cellulose composite films with self-reinforced microfibrils were prepared. The chemical analysis results showed that extracted cellulose microfibrils had higher cellulose content and lower hemicellulose and lignin contents than the raw fibers. The results derived from the FTIR and NMR analyses confirmed that both lignin and most of the hemicellulose were removed during the chemical process. X-ray diffraction results confirmed the partial transition from cellulose I to II during the preparation of cellulose microfibrils. The regenerated cellulose composite films had lower crystallinity. All samples revealed two-step decomposition behavior with the degradation temperatures of 250 °C for raw fibers, 280 °C for cellulose microfibrils and 240 °C for regenerated cellulose composite film suggesting an enhanced thermal stability of cellulose microfibrils. The SEM results illustrated that most of the microfibrils extracted from century fiber had diameters in the range of 8–14 μm. The micrograph of the surface of the regenerated cellulose composite film displayed the presence of reinforced microfibrils. Fairly optically transparent films were obtained by casting, which could be potentially used as optical components for advanced applications. The notable properties of the regenerated cellulose films are promising for applications in transparent biodegradable packaging purpose as a substitute for PP and PE. In general, regenerated cellulose films due to their excellent tensile properties should have a promising impact in food packaging over the coming years. This paper demonstrated that the Agave fibers under study can be potentially used as raw material for the production of regenerated cellulose films.

## Acknowledgements

The author KOR sincerely acknowledges the Faculty of Engineering and Built Environment, University of Johannesburg, South Africa, for the award of Postdoctoral Research Fellowship. The author AVR thanks the Council of Scientific and Industrial Research of India for the award of an Emeritus Scientist, Scheme [21(0842)11/EMR-II dt:10-05-2011].

## References

Ashok, B., Naresh, S., Reddy, K. O., Madhukar, K., Cai, J., Zhang, L., et al. (2014). Tensile and thermal properties of poly(lactic acid)/eggshell powder composite films. *International Journal of Polymer Analysis and Characterization*, *19*(3), 245–255.

Biswas, A., Saha, B. C., Lawton, J. W., Shogren, R. L., & Willett, J. L. (2006). Process for obtaining cellulose acetate from agricultural by-products. *Carbohydrate Polymers*, *64*(1), 134–137.

Cai, J., & Zhang, L. (2005). Rapid dissolution of cellulose in LiOH/urea and NaOH/urea aqueous solutions. *Macromolecular Bioscience*, *5*(6), 539–548.

Cao, Y., Li, H., Zhang, Y., Zhang, J., & He, J. (2010). Structure and properties of novel regenerated cellulose films prepared from cornhusk cellulose in room temperature ionic liquids. *Journal of Applied Polymer Science*, *116*(1), 547–554.

Capanema, E. A., Balakshin, M. Y., & Kadla, J. F. (2004). A comprehensive approach for quantitative lignin characterization by NMR spectroscopy. *Journal of Agricultural and Food Chemistry*, *52*(7), 1850–1860.

Casas, A., Palomar, J., Alonso, M. V., Oliet, M., Omar, S., & Rodriguez, F. (2012). Comparison of lignin and cellulose solubilities in ionic liquids by COSMO-RS analysis and experimental validation. *Industrial Crops and Products*, *37*(1), 155–163.

Cyras, V. P., Commisso, M. S., Mauri, A. N., & Vazquez, A. (2007). Biodegradable double-layer films based on biological resources: Polyhydroxybutyrate and cellulose. *Journal of Applied Polymer Science*, *106*(2), 749–756.

Ding, H. (1995). *Handbook of plastic industry*. Beijing: Chemical Industry Press.

Eichhorn, S. J. (2011). Cellulose nanowhiskers: Promising materials for advanced applications. *Soft Matter*, *7*(2), 303–315.

Fink, H. P., Weigel, P., Purz, H. J., & Ganster, J. (2001). Structure formation of regenerated cellulose materials from NMMO-solutions. *Progress in Polymer Science*, *26*(9), 1473–1524.

Feng, Y., Ashok, B., Madhukar, K., Zhang, J., Zhang, J., Reddy, K. O., et al. (2014). Preparation and characterization of polypropylene carbonate bio-filler (egg shell powder) composite films. *International Journal of Polymer Analysis and Characterization*, http://dx.doi.org/10.1080/1023666X.2014.953747 (in press)

Fort, D. A., Remsing, R. C., Swatloski, R. P., Moyna, P., Moyna, G., & Rogers, R. D. (2007). Can ionic liquids dissolve wood? Processing and analysis of lignocellulosic materials with 1-*n*-butyl-3-methylimidazolium chloride. *Green Chemistry*, *9*(1), 63–69.

Hameed, N., Guo, Q., Tay, F. H., & Kazarian, S. G. (2011). Blends of cellulose and poly (3-hydroxybutyrate-*co*-3-hydroxyvalerate) prepared from the ionic liquid 1-butyl-3-methylimidazolium chloride. *Carbohydrate Polymers*, *86*(1), 94–104.

Hyden, W. L. (1929). Manufacture and properties of regenerated cellulose films. *Industrial & Engineering Chemistry*, *21*(5), 405–410.

Janardhnan, S., & Sain, M. M. (2007). Isolation of cellulose microfibrils—An enzymatic approach. *BioResources*, *1*(2), 176–188.

Jiang, M., Zhao, M., Zhou, Z., Huang, T., Chen, X., & Wang, Y. (2011). Isolation of cellulose with ionic liquid from steam exploded rice straw. *Industrial Crops and Products*, *33*(3), 734–738.

Johar, N., Ahmad, I., & Dufresne, A. (2012). Extraction, preparation and characterization of cellulose fibres and nanocrystals from rice husk. *Industrial Crops and Products*, *37*(1), 93–99.

Klemm, D., Heublein, B., Fink, H. P., & Bohn, A. (2005). Cellulose: Fascinating biopolymer and sustainable raw material. *Angewandte Chemie International Edition*, *44*(22), 3358–3393.

Klemm, D., Kramer, F., Moritz, S., Lindström, T., Ankerfors, M., Gray, D., et al. (2011). Nanocelluloses: A new family of nature-based materials. *Angewandte Chemie International Edition*, *50*(24), 5438–5466.

Kosan, B., Michels, C., & Meister, F. (2008). Dissolution and forming of cellulose with ionic liquids. *Cellulose*, *15*(1), 59–66.

Lee, S. H., Doherty, T. V., Linhardt, R. J., & Dordick, J. S. (2009). Ionic liquid-mediated selective extraction of lignin from wood leading to enhanced enzymatic cellulose hydrolysis. *Biotechnology and Bioengineering*, *102*(5), 1368–1376.

Li, W., Wu, L., Chen, D., Liu, C., & Sun, R. (2011). DMAP-catalyzed phthalylation of cellulose with phthalic anhydride in [bmim] Cl. *BioResources*, *6*(3), 2375–2385.

Liu, C. F., Sun, R. C., Zhang, A. P., Ren, J. L., Wang, X. A., Qin, M. H., et al. (2007). Homogeneous modification of sugarcane bagasse cellulose with succinic anhydride using a ionic liquid as reaction medium. *Carbohydrate Research*, *342*(7), 919–926.

Liu, C. F., Xu, F., Sun, J. X., Ren, J. L., Curling, S., Sun, R. C., et al. (2006). Physicochemical characterization of cellulose from perennial ryegrass leaves (*Lolium perenne*). *Carbohydrate Research*, *341*(16), 2677–2687.

Lowys, M. P., Desbrieres, J., & Rinaudo, M. (2001). Rheological characterization of cellulosic microfibril suspensions. Role of polymeric additives. *Food Hydrocolloids*, *15*(1), 25–32.

Maheswari, C. U., Reddy, K. O., Muzenda, E., Guduri, B. R., & Rajulu, A. V. (2012). Extraction and characterization of cellulose microfibrils from agricultural residue—*Cocos nucifera* L. *Biomass and Bioenergy*, *46*, 555–563.

McCormick, C. L., Callais, P. A., & Hutchinson, B. H., Jr. (1985). Solution studies of cellulose in lithium chloride and *N,N*-dimethylacetamide. *Macromolecules*, *18*(12), 2394–2401.

Mouro, C. R., Bouchet, B., Pontoire, B., Robert, P., Mazoyer, J., & Buléon, A. (2003). Structural features and potential texturising properties of lemon and maize cellulose microfibrils. *Carbohydrate Polymers*, *53*(3), 241–252.

Msahli, S., Sakli, F., & Drean, J. Y. (2006). Study of textile potential of fibers extracted from Tunisian *Agave americana* L. *AUTEX Research Journal*, *6*(1), 9–13.

Nadji, H., Diouf, P. N., Benaboura, A., Bedard, Y., Riedl, B., & Stevanovic, T. (2009). Comparative study of lignins isolated from Alfa grass (*Stipa tenacissima* L.). *Bioresource Technology*, *100*(14), 3585–3592.

Nakagaito, A. N., & Yano, H. (2005). Novel high-strength biocomposites based on microfibrillated cellulose having nano-order-unit web-like network structure. *Applied Physics A*, *80*(1), 155–159.

Northolt, M. G., Boerstoel, H., Maatman, H., Huisman, R., Veurink, J., & Elzerman, H. (2001). The structure and properties of cellulose fibres spun from an anisotropic phosphoric acid solution. *Polymer*, *42*(19), 8249–8264.

Oh, S. Y., Yoo, D. I., Shin, Y., Kim, H. C., Kim, H. Y., Chung, Y. S., et al. (2005). Crystalline structure analysis of cellulose treated with sodium hydroxide and carbon dioxide by means of X-ray diffraction and FTIR spectroscopy. *Carbohydrate Research*, *340*(15), 2376–2391.

Orts, W. J., Shey, J., Imam, S. H., Glenn, G. M., Guttman, M. E., & Revol, J. F. (2005). Application of cellulose microfibrils in polymer nanocomposites. *Journal of Polymers and the Environment*, *13*(4), 301–306.

Pelissari, F. M., Grossmann, M. V., Yamashita, F., & Pineda, E. A. G. (2009). Antimicrobial, mechanical, and barrier properties of cassava starch–chitosan films incorporated with oregano essential oil. *Journal of Agricultural and Food Chemistry*, *57*(16), 7499–7504.

Pereda, M., Dufresne, A., Aranguren, M. I., & Marcovich, N. E. (2014). Polyelectrolyte films based on chitosan/olive oil and reinforced with cellulose nanocrystals. *Carbohydrate Polymers*, *101*, 1018–1026.

Reddy, K. O., Guduri, B. R., & Rajulu, A. V. (2009). Structural characterization and tensile properties of borassus fruit fibers. *Journal of Applied Polymer Science*, *114*(1), 603–611.

Reddy, K. O., Reddy, K. R. N., Zhang, J., Zhang, J., & Varada Rajulu, A. (2013). Effect of alkali treatment on the properties of Century fiber. *Journal of Natural Fibers*, *10*(3), 282–296.

Sain, M., & Panthapulakkal, S. (2006). Bioprocess preparation of wheat straw fibers and their characterization. *Industrial Crops and Products*, *23*(1), 1–8.

Samir, M. A. S. A., Alloin, F., & Dufresne, A. (2005). Review of recent research into cellulosic whiskers, their properties and their application in nanocomposite field. *Biomacromolecules*, *6*(2), 612–626.

Sèbe, G., Ham-Pichavant, F., Ibarboure, E., Koffi, A. L. C., & Tingaut, P. (2012). Supramolecular structure characterization of cellulose II nanowhiskers produced by acid hydrolysis of cellulose I substrates. *Biomacromolecules*, *13*(2), 570–578.

Segal, L. G. J. M. A., Creely, J. J., Martin, A. E., & Conrad, C. M. (1959). An empirical method for estimating the degree of crystallinity of native cellulose using the X-ray diffractometer. *Textile Research Journal*, *29*(10), 786–794.

Siró, I., & Plackett, D. (2010). Microfibrillated cellulose and new nanocomposite materials: A review. *Cellulose*, *17*(3), 459–494.

Soheilmoghaddam, M., Wahit, M. U., Tuck Whye, W., Ibrahim Akos, N., Heidar Pour, R., & Ali Yussuf, A. (2014). Bionanocomposites of regenerated cellulose/zeolite prepared using environmentally benign ionic liquid solvent. *Carbohydrate Polymers*, *106*, 326–334.

Swatloski, R. P., Spear, S. K., Holbrey, J. D., & Rogers, R. D. (2002). Dissolution of cellose with ionic liquids. *Journal of the American Chemical Society*, *124*(18), 4974–4975.

Taniguchi, T., & Okamura, K. (1998). New films produced from microfibrillated natural fibres. *Polymer International*, *47*(3), 291–294.

Torres, F. G., Troncoso, O. P., Torres, C., Díaz, D. A., & Amaya, E. (2011). Biodegradability and mechanical properties of starch films from Andean crops. *International Journal of Biological Macromolecules*, *48*(4), 603–606.

Wise, L. E., Murphy, M., & D'Addieco, A. A. (1946). Chlorite holocellulose: Its fractionation and bearing on summative wood analysis and on studies on the hemicellulose. *Paper Trade Journal*, *122*(2), 35–43.

Yang, D., Peng, X., Zhong, L., Cao, X., Chen, W., Zhang, X., et al. (2014). Green films from renewable resources: Properties of epoxidized soybean oil plasticized ethyl cellulose films. *Carbohydrate Polymers*, *103*, 198–206.

Yang, H., Yan, R., Chen, H., Lee, D. H., & Zheng, C. (2007). Characteristics of hemicellulose, cellulose and lignin pyrolysis. *Fuel*, *86*(12), 1781–1788.

Zhang, H., Wu, J., Zhang, J., & He, J. (2005). 1-Allyl-3-methylimidazolium chloride room temperature ionic liquid: A new and powerful nonderivatizing solvent for cellulose. *Macromolecules*, *38*(20), 8272–8277.

Zhang, Y. H. P., & Lynd, L. R. (2004). Toward an aggregated understanding of enzymatic hydrolysis of cellulose: Noncomplexed cellulase systems. *Biotechnology and Bioengineering*, *88*(7), 797–824.

Zhang, X., Liu, T., Sreekumar, T. V., Kumar, S., Moore, V. C., Hauge, R. H., et al. (2003). Poly(vinyl alcohol)/SWNT composite film. *Nano Letters*, *3*(9), 1285–1288.

Zhu, S., Wu, Y., Chen, Q., Yu, Z., Wang, C., Jin, S., et al. (2006). Dissolution of cellulose with ionic liquids and its application: A mini-review. *Green Chemistry*, *8*(4), 325–327.